Ab initio Exchange-Correlation Free Energy of the Uniform Electron Gas at Warm Dense Matter Conditions

Simon Groth,[1,*] Tobias Dornheim,[1] Travis Sjostrom,[2] Fionn D. Malone,[3,4] W. M. C. Foulkes,[3] and Michael Bonitz[1]

[1]*Institut für Theoretische Physik und Astrophysik, Christian-Albrechts-Universität zu Kiel, D-24098 Kiel, Germany*
[2]*Theoretical Division, Los Alamos National Laboratory, Los Alamos, New Mexico 87545, USA*
[3]*Department of Physics, Imperial College London, Exhibition Road, London SW7 2AZ, United Kingdom*
[4]*Physics Division, Lawrence Livermore National Laboratory, 7000 East Avenue, Livermore, California 94550, USA*

In a recent Letter [T. Dornheim *et al.*, Phys. Rev. Lett. **117**, 156403 (2016)], we presented the first quantum Monte Carlo (QMC) results for the warm dense electron gas in the thermodynamic limit. However, a complete parametrization of the exchange-correlation free energy with respect to density, temperature, and spin polarization remained out of reach due to the absence of (i) accurate QMC results below $\theta = k_B T / E_F = 0.5$ and (ii) QMC results for spin polarizations different from the paramagnetic case. Here we overcome both remaining limitations. By closing the gap to the ground state and by performing extensive QMC simulations for different spin polarizations, we are able to obtain the first completely *ab initio* exchange-correlation free energy functional; the accuracy achieved is an unprecedented ∼0.3%. This also allows us to quantify the accuracy and systematic errors of various previous approximate functionals.

The past decade has witnessed a rapid growth of interest in matter under extreme excitation or compression, as in laser-excited solids [1] and inertial confinement fusion targets [2–5]. Astrophysical examples such as white dwarf atmospheres and planet interiors [6,7] provide further motivation. More down-to-earth examples appear in radiation damage cascades in the walls of fission or fusion reactors [8]. Plasmonic catalysts use hot electrons created by the decay of plasmons in otherwise cold metallic nanoparticles to accelerate chemical reactions [9,10]. Systems such as these, with thermal energies $k_B T$ comparable to the Fermi energy E_F and densities comparable to or greater than those of ordinary solids, are said to be in the "warm dense matter" (WDM) regime [11]. Because the degeneracy parameter $\Theta = k_B T / E_F$ is of the order of unity, neither the Pauli exclusion principle nor electronic excitations can be ignored and there are no small parameters in which to expand. This makes WDM challenging to understand theoretically.

The density functional theory (DFT) is by far the most important computational approach used to study molecules and solids at low temperatures [12–14] but relies for its success on the availability of good approximations to the unknown exchange-correlation (XC) energy functional. The development in the early 1980s of accurate parametrizations [15,16] of the ground-state local density approximation to this functional played a decisive role in the ensuing rise of the DFT.

The DFT was generalized to finite temperatures [17] soon after its invention, but applications to warm dense systems are a recent development. In part, this is because the finite-temperature equivalent of the local density approximation is not known accurately. This Letter presents the first accurate and fully *ab initio* calculation and parametrization of the XC free energy per electron, $f_{\rm xc}$, as a functional of the temperature, density, and spin polarization, covering the entire range of conditions of interest in applications. The result is the natural generalization of Perdew and Zunger's famous zero-temperature functional [16]. It is key input not only to the thermal DFT [17–19] but also for quantum hydrodynamics [20,21] and the construction of equations of state for astrophysical objects [22–24].

The local density approximation is based on properties of the uniform electron gas (UEG), one of the seminal model systems in physics [25]. Studies of the UEG led to key insights such as the Fermi liquid theory [26,27], the quasiparticle picture of collective excitations [28,29], and the theory of superconductivity [30]. Accurate parametrizations of its ground-state properties [15,16,31–34] based on quantum Monte Carlo (QMC) simulations [35–39] have sparked many applications [40–42] in addition to facilitating the remarkable successes of the DFT [12–14].

QMC methods for the warm dense electron gas are much less developed, so the first parametrizations of $f_{\rm xc}$ were based instead on uncontrolled approximations such as interpolations between known limits [43], semiempirical quantum-classical mappings [41,44], and dielectric (linear response) methods [45–49]. To overcome the severe limitations imposed by the fermion sign problem [50,51], the pioneering QMC simulations of the UEG by Brown *et al.* [52] used the approximate restricted path integral Monte Carlo (RPIMC) approach, in which the nodal structure of the density matrix is assumed. These data were used as input for several parametrizations of $f_{\rm xc}$ [46,53,54],
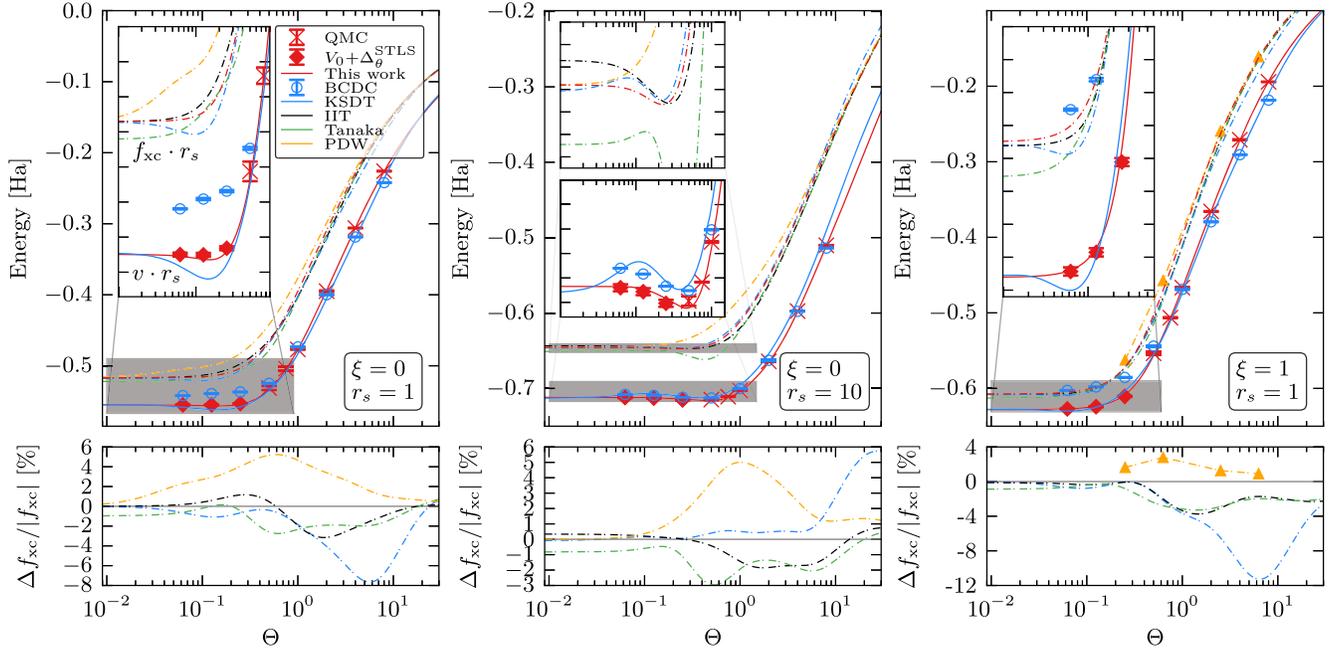
FIG. 1.   Temperature dependence of the XC free energy and potential energy—the top row shows f_{xc} (dashed lines) from this work (red), KSDT (blue [53]), IIT (black [48,49]), Tanaka (green [47]), and Perrot–Dharma-wardana (yellow dashed line and triangles, PDW [44]), as well as the corresponding interaction energy v (solid lines) from this work, KSDT, and the restricted PIMC results by Brown *et al.* (blue dots [52]). The red rhombs correspond to ground-state QMC results plus a temperature correction function obtained from the STLS theory. The inset corresponds to an enlargement of the gray box. The bottom row displays the relative deviations of the different models of f_{xc} with respect to our new parametrization.

the most sophisticated being that of Karasiev, Sjostrom, Dufty, and Trickey (KSDT) [53], but were later shown to be inaccurate [55]. The errors were $\sim 10\%$ near $r_s = 1$, where $r_s \equiv \bar{r}/a_B$, $\bar{r}$ is the radius of a sphere containing one electron on average, and a_B is the Bohr radius. Unsurprisingly, the aforementioned models for f_{xc} disagree substantially (cf. Fig. 1) in the WDM regime [56].

This unsatisfactory situation has sparked much recent work on finite-temperature fermionic QMC algorithms [55,57–65]. By developing three complementary new methods—configuration PIMC [55], permutation blocking PIMC [62,63], and density matrix QMC [64,65]—we are now able to overcome the sign problem in a broad parameter range without relying on a fixed-node approximation [66,67]. In a recent Letter [61], we presented an improved procedure to extrapolate the QMC results to the thermodynamic limit and thereby obtained data for the unpolarized UEG with an unprecedented accuracy of the order of 0.1%. At that time, however, the construction of a complete parametrization of f_{xc} with respect to r_s, θ, and $\xi = (N^\uparrow - N^\downarrow)/(N^\uparrow + N^\downarrow)$, where $N^\uparrow$ ($N^\downarrow$) is the number of spin-up (spin-down) electrons, was not possible. The fermion sign problem prevented us from performing QMC simulations for $0 < \theta < 0.5$. Further, we had no results for spin polarizations other than $\xi = 0$. The polarization dependence of f_{xc} is used, for example, in DFT calculations in the local spin-density approximation, which require the evaluation of f_{xc} at arbitrary ξ.

Here we solve these problems and present a new functional. Inspired by Tanaka and Ichimaru [48,49] and the impressive accuracy of the Singwi-Tosi-Land-Sjölander (STLS) formalism [45,46] in the warm dense regime [56], we bridge the gap between $\theta = 0$ and $\theta = 0.25$ by adding the (small) temperature dependence of the STLS interaction energy,

$$\Delta_\theta^{\text{STLS}}(r_s, \theta, \xi) := v^{\text{STLS}}(r_s, \theta, \xi) - v^{\text{STLS}}(r_s, 0, \xi), \quad (1)$$

to the ground-state QMC interaction energy, which is known very accurately [39]. Second, we carry out extensive QMC simulations of the warm dense UEG for $\xi = 1/3, 0.6$, and 1 (179 data points in the ranges $0.1 \leq r_s \leq 20$ and $0.5 \leq \theta \leq 8$; see Table III in the Supplemental Material [68]). In combination with the results from Ref. [61], this allows us to construct the first complete *ab initio* parametrization of the XC free energy, $f_{xc}(r_s, \theta, \xi)$, and to attain an unprecedented accuracy of $\sim 0.3\%$. The high quality of our new results is verified by various cross-checks and compared to the widely used parametrizations by KSDT [53], Perrot and Dharma-wardana [44], Ichimaru, Iyetomi, and Tanaka (IIT [48,49]), and the recent improved dielectric approach by Tanaka [47].

Parametrization of f_{xc} for $\xi = 0$ and $\xi = 1$.—Following Refs. [48,49], we obtain f_{xc}^ξ from our QMC data for the electron-electron interaction energy $v^\xi(r_s, \theta)$ via the coupling-constant integration formula

$$f_{\mathrm{xc}}^{\xi}(r_s,\theta) = \frac{1}{r_s^2}\int_0^{r_s} d\bar{r}_s \bar{r}_s v^{\xi}(\bar{r}_s,\theta) \qquad (2)$$

$$\Rightarrow v^{\xi}(r_s,\theta) = 2f_{\mathrm{xc}}^{\xi}(r_s,\theta) + r_s \left.\frac{\partial f_{\mathrm{xc}}^{\xi}(r_s,\theta)}{\partial r_s}\right|_{\theta}. \qquad (3)$$

We employ Padé representations of f_{xc}^1 and f_{xc}^0 (see Supplemental Material [68], which includes Refs. [69,70]) and fit the right-hand side of Eq. (3) to our combined data for $v^{1,0}$. To ensure the correct ground-state behavior, we note that $\lim_{\theta\to 0} f_{\mathrm{xc}}^{\xi}(r_s,\theta) = e_{\mathrm{xc}}^{\xi}(r_s,0)$ and fit the zero-temperature limit of our Padé formula to the recent ground-state QMC results of Spink, Needs, and Drummond [39]. In addition, the classical Debye-Hückel limit for large θ and the Hartree-Fock limit $f_{\mathrm{xc}}^{\mathrm{HF}}(r_s,\theta) = a(\theta)/r_s \equiv a^{\mathrm{HF}}(\theta)/r_s$ [71] for $r_s \to 0$ are exactly incorporated.

The new results for $f_{\mathrm{xc}}^{\xi}(r_s,\theta)$ are depicted in Fig. 1 (red dashed line) and compared to various approximations. While all curves exhibit a qualitatively similar behavior with respect to the temperature, there are deviations of 5%–12% for intermediate θ (bottom row). The IIT parametrization exhibits the smallest errors when $\xi = 0$, whereas, for $\xi = 1$, the Perrot–Dharma-wardana points are superior, although the IIT curve is of a similar quality. The recent parametrization by Tanaka (green) does not constitute an improvement compared to IIT. Finally, the KSDT curves are relatively accurate at low θ but systematically deviate for $\theta \gtrsim 0.5$, especially at a high density ($r_s \lesssim 4$ [68]). The deviation of $\Delta f/f \sim 10\%$ at its maximum can be traced to an inappropriate finite-size correction of the QMC data by Brown *et al.* [52]; see Ref. [61]. The deviations are even more severe for $\xi = 1$, in agreement with previous findings about the systematic bias in the RPIMC input data [66,67] and with recent investigations [47,49] of f_{xc} itself. Also notice the pronounced bump of f_{xc}^0 occurring for large r_s and a low temperature (see the inset in the middle panel), which induces an unphysical negative total entropy [72] in the KSDT fit.

Consider now our results for the interaction energy, shown as red rhombs and crosses in Fig. 1. We observe a smooth connection between our QMC data for $\theta \geq 0.5$ (crosses) and the temperature-corrected ground-state data (rhombs) in all three parts of the figure. The connection is equally smooth at all other densities investigated. The solid red line depicts the fit to v^{ξ} [Eq. (3)]. The Padé ansatz proves an excellent fitting function, able to reproduce the input data (v^{ξ}) for $\xi = 0$ ($\xi = 1$) with a mean and maximum deviation of 0.12% and 0.68% (0.17% and 0.63%), respectively [73].

To further illustrate the high quality of our XC functional and to verify the accuracy of the applied temperature correction at low θ, we carried out extensive new QMC simulations for the XC internal energy per particle, e_{xc}, for $r_s = 1$ and $\xi = 1$, over the entire range of temperatures down to $\theta = 0.0625$ (see Ref. [68] for details). The
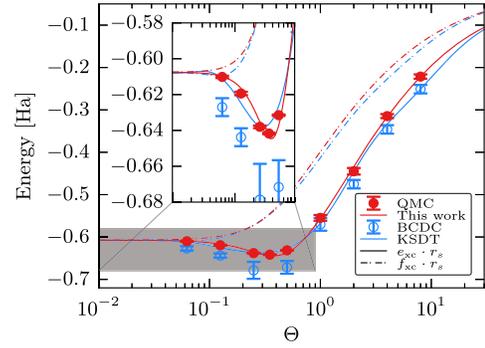

FIG. 2. Cross-check of our parametrization ($\xi = 1$, $r_s = 1$). The XC energy per electron (red line), as calculated from our Padé function for f_{xc} (dashed line), is compared to new, independent finite-size-corrected QMC data (red dots) [68]. While our functional has been constructed solely using the interaction energy v [cf. Eq. (3)], the KSDT curve [53] (solid blue) was fitted to the restricted PIMC data [52] for e_{xc} (blue circles, BCDC).

finite-size-corrected data are compared to e_{xc} reconstructed from our parametrization of $f_{\mathrm{xc}}^{\xi}(r_s,\theta)$ via [53]

$$e_{\mathrm{xc}}^{\xi}(r_s,\theta) = f_{\mathrm{xc}}^{\xi}(r_s,\theta) - \theta \left.\frac{\partial f_{\mathrm{xc}}^{\xi}(r_s,\theta)}{\partial \theta}\right|_{r_s}. \qquad (4)$$

This allows us to gauge not only the accuracy of f_{xc} itself but also its temperature derivative, which is directly linked to the XC entropy. The results are presented in Fig. 2 and demonstrate excellent agreement between our parametrization (red solid line) and the independent new QMC data (red dots) over the entire range of θ. Since the new data for e_{xc} were not used for our fit, this constitutes a strong confirmation of the accuracy of the low-temperature results obtained by using the STLS theory to correct the $T = 0$ XC energy and demonstrates the consistency of our parametrization. Other functionals are much less consistent (see blue symbols and line) [73,74].

Spin interpolation.—To obtain an accurate parametrization of f_{xc} at arbitrary spin polarization $0 \leq \xi \leq 1$, we employ the ansatz [44]

$$f_{\mathrm{xc}}(r_s,\theta,\xi) = f_{\mathrm{xc}}^0(r_s,\theta^0) + [f_{\mathrm{xc}}^1(r_s,\theta^0 \cdot 2^{-2/3}) - f_{\mathrm{xc}}^0(r_s,\theta^0)]\Phi(r_s,\theta^0,\xi), \qquad (5)$$

with $\theta^0 = \theta(1 + \xi)^{2/3}$. The form and fitting procedure used for the interpolation function $\Phi(r_s,\theta^0,\xi)$ are described in the Supplemental Material [68]. Interestingly, we find that a single fitting parameter is sufficient to capture the full temperature dependence of Φ for all values of ξ, with a mean and maximum deviation from the QMC data at intermediate ξ of 0.15% and 0.8%, respectively.

Note that this is the first time that $\Phi(r_s,\theta,\xi)$ has been obtained accurately from *ab initio* data. A comparison of the
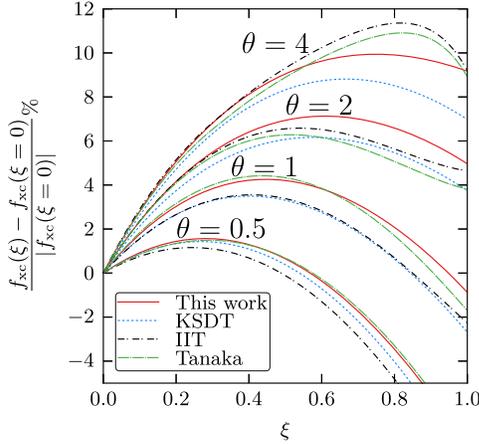
FIG. 3. Dependence of the XC free energy on spin polarization at $r_s = 1$. The *ab initio* functional derived here (red curve) is compared to the parametrizations of KSDT (blue curve) [53], IIT (black curve) [48,49], and Tanaka (green curve) [47].

ξ dependence of f_{xc} with various earlier parametrizations is depicted in Fig. 3. The IIT and Tanaka curves, which utilize a different functional form for the spin interpolation [75], exhibit the largest deviations at intermediate temperatures. Our spin-interpolation function has the same form [68] as that employed in the KSDT parametrization. However, due to the absence of restricted PIMC data for intermediate ξ, KSDT used the classical mapping of Ref. [44] to determine the coefficients of Φ. Overall, the KSDT fit is closest to our parametrization at low θ, while for $\theta > 1$ the IIT curve is more accurate. Nevertheless, we conclude that no previous model satisfactorily captures the ξ dependence uncovered by our data.

Summary and discussion.—In summary, we have presented the first accurate and fully *ab initio* XC free energy functional for the UEG at WDM conditions, achieving an unprecedented precision of $\Delta f_{\mathrm{xc}}/f_{\mathrm{xc}} \sim 0.3\%$. To cover the entire parameter range relevant to experiments, we carried out extensive QMC simulations for multiple spin polarizations at $0.1 \leq r_s \leq 20$ and $0.5 \leq \theta \leq 8$. In addition, we obtained accurate data for $0.0625 \leq \theta \leq 0.25$ by combining ground-state QMC results with a small STLS-based temperature correction. All of our results are tabulated in the Supplemental Material [68] and provide benchmarks for the development of new theories and simulation schemes as well as for the improvement of existing models.

The first step in our construction of the complete XC functional, $f_{\mathrm{xc}}(r_s, \theta, \xi)$, was to parametrize the completely polarized and unpolarized cases. This was achieved by fitting the right-hand side of Eq. (3) to our new data for the interaction energy, v^ξ, for $\xi = 0$ and $\xi = 1$. The resulting parametrization reproduces the input data with a mean deviation of 0.17%, better by at least an order of magnitude than the KSDT fit. As an additional test of our parametrization, we performed independent QMC calculations of e_{xc} (the XC energy per electron) for a wide range of values of θ

down to $\theta = 0.0625$ and compared the results with values of e_{xc} calculated using our functional for f_{xc}. The striking agreement obtained constitutes strong evidence for the accuracy of the STLS-based corrections used at a low temperature and for the consistency of our work, in general.

Equipped with our new XC functional, we have also investigated the systematic errors of previous parametrizations. Overall, the functional by Ichimaru, Iyetomi, and Tanaka [48,49] deviates the least from our results, although at $\xi = 1$ the classical mapping results by Perrot and Dharma-wardana [44] are similarly accurate. The KSDT parametrization exhibits large deviations exceeding 10% at a high temperature and density. At low temperatures, however, it performs surprisingly well, in part because it does not reproduce the systematic biases in the restricted PIMC data on which it was based.

The construction of the first *ab initio* spin-interpolation function $\Phi(r_s, \theta, \xi)$ at WDM conditions constitutes the capstone of this work. Surprisingly, we find that a one-parameter fit is sufficient to capture the whole temperature dependence of the spin-interpolation function. Furthermore, we show that no previously suggested spin interpolation gives the correct ξ dependence throughout the WDM regime.

We are confident that our extensive QMC data set and accurate parametrization of the thermodynamic functions of the warm dense electron gas will be useful in many applications. Given recent developments in the thermal Kohn-Sham DFT [76,77], time-dependent Kohn-Sham DFT [78], and orbital-free DFT [79,80], our parametrization of f_{xc} is directly applicable for calculations in the local spin-density approximation. Furthermore, our functional can be used as a basis for gradient expansions [81,82] or as a benchmark for nonlocal functionals based on the fluctuation-dissipation theorem [83]. In addition, it can be straightforwardly incorporated into widely used approximations in quantum hydrodynamics [20,21] or for the equations of state of astrophysical objects [22–24]. Finally, our XC functional should help resolve several exciting and controversial issues in warm dense matter physics, such as the existence and locations of the phase transitions in warm dense hydrogen [84–86] or details of hydrogen-helium demixing [87].

Computational implementations of our XC functional (in FORTRAN, C++, and PYTHON) are available online [88].

P H Y S I C A L R E V I E W L E T T E R S

---

*groth@theo-physik.uni-kiel.de

[1] R. Ernstorfer, M. Harb, C. T. Hebeisen, G. Sciaini, T. Dartigalongue, and R. J. D. Miller, The formation of warm dense matter: Experimental evidence for electronic bond hardening in gold, Science **323**, 1033 (2009).

[2] R. Nora *et al.*, Gigabar Spherical Shock Generation on the OMEGA Laser, Phys. Rev. Lett. **114**, 045001 (2015).

[3] P. F. Schmit *et al.*, Understanding Fuel Magnetization and Mix Using Secondary Nuclear Reactions in Magneto-Inertial Fusion, Phys. Rev. Lett. **113**, 155004 (2014).

[4] O. A. Hurricane *et al.*, Inertially confined fusion plasmas dominated by alpha-particle self-heating, Nat. Phys. **12**, 800 (2016).

[5] A. L. Kritcher, T. Döppner, C. Fortmann, T. Ma, O. L. Landen, R. Wallace, and S. H. Glenzer, In-Flight Measurements of Capsule Shell Adiabats in Laser-Driven Implosions, Phys. Rev. Lett. **107**, 015002 (2011).

[6] M. D. Knudson, M. P. Desjarlais, R. W. Lemke, T. R. Mattsson, M. French, N. Nettelmann, and R. Redmer, Probing the Interiors of the Ice Giants: Shock Compression of Water to 700 GPa and 3.8 g/cm^3, Phys. Rev. Lett. **108**, 091102 (2012).

[7] B. Militzer, W. B. Hubbard, J. Vorberger, I. Tamblyn, and S. A. Bonev, A massive core in Jupiter predicted from first-principles simulations, Astrophys. J. **688**, L45 (2008).

[8] E. Zarkadoula, S. L. Daraszewicz, D. M. Duffy, M. A. Seaton, I. T. Todorov, K. Nordlund, M. T. Dove, and K. Trachenko, Electronic effects in high-energy radiation damage in iron, J. Phys. Condens. Matter **26**, 085401 (2014).

[9] S. Mukherjee, F. Libisch, N. Large, O. Neumann, L. V. Brown, J. Cheng, J. Britt Lassiter, E. A. Carter, P. Nordlander, and N. J. Halas, Hot electrons do the impossible: Plasmon-induced dissociation of H_2 on Au, Nano Lett. **13**, 240 (2013).

[10] M. L. Brongersma, N. J. Halas, and P. Nordlander, Plasmon-induced hot carrier science and technology, Nat. Nanotechnol. **10**, 25 (2015).

[11] F. Graziani, M. P. Desjarlais, R. Redmer, and S. B. Trickey, *Frontiers and Challenges in Warm Dense Matter* (Springer, New York, 2014).

[12] W. Kohn and L. J. Sham, Self-consistent equations including exchange and correlation effects, Phys. Rev. **140**, A1133 (1965).

[13] R. O. Jones, Density functional theory: Its origins, rise to prominence, and future, Rev. Mod. Phys. **87**, 897 (2015).

[14] K. Burke, Perspective on density functional theory, J. Chem. Phys. **136**, 150901 (2012).

[15] S. H. Vosko, L. Wilk, and M. Nusair, Accurate spin-dependent electron liquid correlation energies for local spin density calculations: A critical analysis, Can. J. Phys. **58**, 1200 (1980).

[16] J. P. Perdew and A. Zunger, Self-interaction correction to density-functional approximations for many-electron systems, Phys. Rev. B **23**, 5048 (1981).

[17] N. D. Mermin, Thermal properties of the inhomogeneous electron gas, Phys. Rev. **137**, A1441 (1965).

[18] B. Holst, M. French, and R. Redmer, Electronic transport coefficients from *ab initio* simulations and application to dense liquid hydrogen, Phys. Rev. B **83**, 235120 (2011).

[19] J. C. Smith, F. Sagredo, and K. Burke, Warming up density functional theory, arXiv:1701.00873.

[20] N. Crouseilles, P.-A. Hervieux, and G. Manfredi, Quantum hydrodynamic model for the nonlinear electron dynamics in thin metal films, Phys. Rev. B **78**, 155412 (2008).

[21] D. Michta, F. Graziani, and M. Bonitz, Quantum hydro-dynamics for plasmas—A Thomas-Fermi theory perspective, Contrib. Plasma Phys. **55**, 437 (2015).

[22] A. Y. Potekhin and G. Chabrier, Equation of state for magnetized Coulomb plasmas, Astron. Astrophys. **550**, A43 (2013).

[23] D. Saumon, G. Chabrier, and H. M. van Horn, An equation of state for low-mass stars and giant planets, Astrophys. J. Suppl. Ser. **99**, 713 (1995).

[24] A. Becker, W. Lorenzen, J. J. Fortney, N. Nettelmann, M. Schöttler, and R. Redmer, *Ab initio* equations of state for hydrogen (H-REOS.3) and helium (He-REOS.3) and their implications for the interior of brown dwarfs, Astrophys. J. Suppl. Ser. **215**, 21 (2014).

[25] P.-F. Loos and P. M. W. Gill, The uniform electron gas, Comput. Mol. Sci. **6**, 410 (2016).

[26] G. Giuliani and G. Vignale, *Quantum Theory of the Electron Liquid* (Cambridge University Press, Cambridge, England, 2008).

[27] G. Baym and C. Pethick, *Landau Fermi-Liquid Theory: Concepts and Applications* (Wiley, New York, 1991).

[28] D. Pines and D. Bohm, A collective description of electron interactions: II. collective vs individual particle aspects of the interactions, Phys. Rev. **85**, 338 (1952).

[29] D. Bohm and D. Pines, A collective description of electron interactions: III. Coulomb interactions in a degenerate electron gas, Phys. Rev. **92**, 609 (1953).

[30] J. Bardeen, L. N. Cooper, and J. R. Schrieffer, Theory of superconductivity, Phys. Rev. **108**, 1175 (1957).

[31] J. P. Perdew and Y. Wang, Pair-distribution function and its coupling-constant average for the spin-polarized electron gas, Phys. Rev. B **46**, 12947 (1992).

[32] M. Corradini, R. Del Sole, G. Onida, and M. Palummo, Analytical expressions for the local-field factor $G(q)$ and the exchange-correlation kernel $K_{xc}(r)$ of the homogeneous electron gas, Phys. Rev. B **57**, 14569 (1998).

[33] P. Gori-Giorgi, F. Sacchetti, and G. B. Bachelet, Analytic static structure factors and pair-correlation functions for the unpolarized homogeneous electron gas, Phys. Rev. B **61**, 7353 (2000).

[34] P. Gori-Giorgi and J. P. Perdew, Pair distribution function of the spin-polarized electron gas: A first-principles analytic model for all uniform densities, Phys. Rev. B **66**, 165118 (2002).

[35] D. M. Ceperley, Ground state of the fermion one-component plasma: A Monte Carlo study in two and three dimensions, Phys. Rev. B **18**, 3126 (1978).

[36] D. M. Ceperley and B. J. Alder, Ground State of the Electron Gas by a Stochastic Method, Phys. Rev. Lett. **45**, 566 (1980).

[37] G. Ortiz and P. Ballone, Correlation energy, structure factor, radial distribution function, and momentum distribution of the spin-polarized uniform electron gas, Phys. Rev. B **50**, 1391 (1994).

[38] G. Ortiz, M. Harris, and P. Ballone, Zero Temperature Phases of the Electron Gas, Phys. Rev. Lett. **82**, 5317 (1999).

[39] G. G. Spink, R. J. Needs, and N. D. Drummond, Quantum Monte Carlo study of the three-dimensional spin-polarized homogeneous electron gas, Phys. Rev. B **88**, 085121 (2013).

[40] B. Farid, V. Heine, G. E. Engel, and I. J. Robertson, Extremal properties of the Harris-Foulkes functional and an improved screening calculation for the electron gas, Phys. Rev. B **48**, 11602 (1993).

[41] M. W. C. Dharma-wardana and F. Perrot, Simple Classical Mapping of the Spin-Polarized Quantum Electron Gas: Distribution Functions and Local-Field Corrections, Phys. Rev. Lett. **84**, 959 (2000).

[42] Y. Takada, Emergence of an excitonic collective mode in the dilute electron gas, Phys. Rev. B **94**, 245106 (2016).

[43] W.-D. Kraeft, D. Kremp, W. Ebeling, and G. Röpke, *Quantum Statistics of Charged Particle Systems* (Akademie-Verlag, Berlin, 1986).

[44] F. Perrot and M. W. C. Dharma-wardana, Spin-polarized electron liquid at arbitrary temperatures: Exchange-correlation energies, electron-distribution functions, and the static response functions, Phys. Rev. B **62**, 16536 (2000).

[45] S. Tanaka and S. Ichimaru, Thermodynamics and correlational properties of finite-temperature electron liquids in the Singwi-Tosi-Land-Sjölander approximation, J. Phys. Soc. Jpn. **55**, 2278 (1986).

[46] T. Sjostrom and J. Dufty, Uniform electron gas at finite temperatures, Phys. Rev. B **88**, 115123 (2013).

[47] S. Tanaka, Correlational and thermodynamic properties of finite-temperature electron liquids in the hypernetted-chain approximation, J. Chem. Phys. **145**, 214104 (2016).

[48] S. Ichimaru, H. Iyetomi, and S. Tanaka, Statistical physics of dense plasmas: Thermodynamics, transport coefficients and dynamic correlations, Phys. Rep. **149**, 91 (1987).

[49] S. Tanaka, Improved equation of state for finite-temperature spin-polarized electron liquids on the basis of Singwi-Tosi-Land-Sjolander approximation, Contrib. Plasma Phys. **57**, 126 (2017).

[50] E. Y. Loh, J. E. Gubernatis, R. T. Scalettar, S. R. White, D. J. Scalapino, and R. L. Sugar, Sign problem in the numerical simulation of many-electron systems, Phys. Rev. B **41**, 9301 (1990).

[51] M. Troyer and U. J. Wiese, Computational Complexity and Fundamental Limitations to Fermionic Quantum Monte Carlo Simulations, Phys. Rev. Lett. **94**, 170201 (2005).

[52] E. W. Brown, B. K. Clark, J. L. DuBois, and D. M. Ceperley, Path-Integral Monte Carlo Simulation of the Warm Dense Homogeneous Electron Gas, Phys. Rev. Lett. **110**, 146405 (2013).

[53] V. V. Karasiev, T. Sjostrom, J. Dufty, and S. B. Trickey, Accurate Homogeneous Electron Gas Exchange-Correlation Free Energy for Local Spin-Density Calculations, Phys. Rev. Lett. **112**, 076403 (2014).

[54] E. W. Brown, J. L. DuBois, M. Holzmann, and D. M. Ceperley, Exchange-correlation energy for the three-dimensional homogeneous electron gas at arbitrary temperature, Phys. Rev. B **88**, 081102(R) (2013).

[55] T. Schoof, S. Groth, J. Vorberger, and M. Bonitz, *Ab Initio* Thermodynamic Results for the Degenerate Electron Gas at Finite Temperature, Phys. Rev. Lett. **115**, 130402 (2015).

[56] S. Groth, T. Dornheim, and M. Bonitz, Free energy of the uniform electron gas: Testing analytical models against first principle results, Contrib. Plasma Phys. **57**, 137 (2017).

[57] V. Filinov, V. Fortov, M. Bonitz, and Zh. Moldabekov, Fermionic path integral Monte Carlo results for the uniform electron gas at finite temperature, Phys. Rev. E **91**, 033108 (2015).

[58] J. L. DuBois, E. W. Brown, and B. J. Alder, Overcoming the fermion sign problem in homogeneous systems, arXiv:1409.3262.

[59] T. Schoof, M. Bonitz, A. V. Filinov, D. Hochstuhl, and J. W. Dufty, Configuration path integral Monte Carlo, Contrib. Plasma Phys. **51**, 687 (2011).

[60] T. Dornheim, S. Groth, F. D. Malone, T. Schoof, T. Sjostrom, W. M. C. Foulkes, and M. Bonitz, *Ab initio* quantum Monte Carlo simulation of the warm dense electron gas, Phys. Plasmas **24**, 056303 (2017).

[61] T. Dornheim, S. Groth, T. Sjostrom, F. D. Malone, W. M. C. Foulkes, and M. Bonitz, *Ab Initio* Quantum Monte Carlo Simulation of the Warm Dense Electron Gas in the Thermodynamic Limit, Phys. Rev. Lett. **117**, 156403 (2016).

[62] T. Dornheim, S. Groth, A. Filinov, and M. Bonitz, Permutation blocking path integral Monte Carlo: A highly efficient approach to the simulation of strongly degenerate non-ideal fermions, New J. Phys. **17**, 073017 (2015).

[63] T. Dornheim, T. Schoof, S. Groth, A. Filinov, and M. Bonitz, Permutation blocking path integral Monte Carlo approach to the uniform electron gas at finite temperature, J. Chem. Phys. **143**, 204101 (2015).

[64] F. D. Malone, N. S. Blunt, J. J. Shepherd, D. K. K. Lee, J. S. Spencer, and W. M. C. Foulkes, Interaction picture density matrix quantum Monte Carlo, J. Chem. Phys. **143**, 044116 (2015).

[65] F. D. Malone, N. S. Blunt, E. W. Brown, D. K. K. Lee, J. S. Spencer, W. M. C. Foulkes, and J. J. Shepherd, Accurate Exchange-Correlation Energies for the Warm Dense Electron Gas, Phys. Rev. Lett. **117**, 115701 (2016).

[66] S. Groth, T. Schoof, T. Dornheim, and M. Bonitz, *Ab initio* quantum Monte Carlo simulations of the uniform electron gas without fixed nodes, Phys. Rev. B **93**, 085102 (2016).

[67] T. Dornheim, S. Groth, T. Schoof, C. Hann, and M. Bonitz, *Ab initio* quantum Monte Carlo simulations of the uniform electron gas without fixed nodes: The unpolarized case, Phys. Rev. B **93**, 205134 (2016).

[68] See Supplemental Material at http://link.aps.org/supplemental/10.1103/PhysRevLett.119.135001 for additional information and data tables.

[69] N. D. Drummond, R. J. Needs, A. Sorouri, and W. M. C. Foulkes, Finite-size errors in continuum quantum Monte Carlo calculations, Phys. Rev. B **78**, 125106 (2008).

[70] C. Lin, F. H. Zong, and D. M. Ceperley, Twist-averaged boundary conditions in continuum quantum Monte Carlo algorithms, Phys. Rev. E **64**, 016702 (2001).

[71] F. Perrot and M. W. C. Dharma-wardana, Exchange and correlation potentials for electron-ion systems at finite temperatures, Phys. Rev. A **30**, 2619 (1984).

[72] K. Burke, J. C. Smith, P. E. Grabowski, and A. Pribram-Jones, Exact conditions on the temperature dependence of density functionals, Phys. Rev. B **93**, 195132 (2016).

[73] In contrast, the KSDT interaction energy (solid blue line) exhibits severe deviations to the corresponding data by Brown *et al.* [52] (blue dots). This indicates that using the systematically biased restricted PIMC data as input for a parametrization of f_{xc} does not allow one to consistently recover other quantities (see also the discussion of Fig. 2).

[74] Note that the KSDT parametrization is the result of a direct fit to the restricted PIMC data for e_{xc} but reproduces these data only for $\theta \geq 1$ and strongly deviates below (the KSDT fit exhibits a mean and maximum deviation to the underlying restricted PIMC data of 1.2% and 7.8% for $\xi = 1$).

[75] S. Tanaka and S. Ichimaru, Spin-dependent correlations and thermodynamic functions for electron liquids at arbitrary degeneracy and spin polarization, Phys. Rev. B **39**, 1036 (1989).

[76] S. Zhang, H. Wang, W. Kang, P. Zhang, and X. T. He, Extended application of Kohn-Sham first-principles molecular dynamics method with plane wave approximation at high energy—From cold materials to hot dense plasmas, Phys. Plasmas **23**, 042707 (2016).

[77] C. Gao, S. Zhang, W. Kang, C. Wang, P. Zhang, and X. T. He, Validity boundary of orbital-free molecular dynamics method corresponding to thermal ionization of shell structure, Phys. Rev. B **94**, 205115 (2016).

[78] A. D. Baczewski, L. Shulenburger, M. P. Desjarlais, S. B. Hansen, and R. J. Magyar, X-Ray Thomson Scattering in Warm Dense Matter without the Chihara Decomposition, Phys. Rev. Lett. **116**, 115004 (2016).

[79] T. Sjostrom and J. Daligault, Fast and Accurate Quantum Molecular Dynamics of Dense Plasmas Across Temperature Regimes, Phys. Rev. Lett. **113**, 155006 (2014).

[80] V. V. Karasiev, T. Sjostrom, and S. B. Trickey, Finite-temperature orbital-free DFT molecular dynamics: Coupling Profess and Quantum Espresso, Comput. Phys. Commun. **185**, 3240 (2014).

[81] T. Sjostrom and J. Daligault, Gradient corrections to the exchange-correlation free energy, Phys. Rev. B **90**, 155109 (2014).

[82] V. V. Karasiev, J. W. Dufty, and S. B. Trickey, Nonempirical semi-local free-energy density functional for warm dense matter, arXiv:1612.06266.

[83] A. Pribram-Jones, P. E. Grabowski, and K. Burke, Thermal Density Functional Theory: Time-Dependent Linear Response and Approximate Functionals from the Fluctuation-Dissipation Theorem, Phys. Rev. Lett. **116**, 233001 (2016).

[84] G. Norman and A. Starostin, Insufficiency of classical description of a nondegenerate dense plasma, High Temp. **6**, 394399 (1968).

[85] V. E. Fortov, R. I. Ilkaev, V. A. Arinin, V. V. Burtzev, V. A. Golubev, I. L. Iosilevskiy, V. V. Khrustalev, A. L. Mikhailov, M. A. Mochalov, V. Ya. Ternovoi, and M. V. Zhernokletov, Phase Transition in a Strongly Nonideal Deuterium Plasma Generated by Quasi-Isentropical Compression at Megabar Pressures, Phys. Rev. Lett. **99**, 185001 (2007).

[86] C. Pierleoni, M. A. Morales, G. Rillo, M. Holzmann, and D. M. Ceperley, Liquid-liquid phase transition in hydrogen by coupled electron-ion Monte Carlo simulations, Proc. Natl. Acad. Sci. U.S.A. **113**, 4953 (2016).

[87] M. A. Morales, E. Schwegler, D. M. Ceperley, C. Pierleoni, S. Hamel, and K. Caspersen, Phase separation in hydrogen-helium mixtures at Mbar pressures, Proc. Natl. Acad. Sci. U.S.A. **106**, 1324 (2009).

[88] https://github.com/agbonitz/xc_functional.